AAPS PharmSciTech, Vol. 16, No. 5, October 2015 (© 2015)
DOI: 10.1208/s12249-015-0298-9

Research Article

Design of Micelle Nanocontainers Based on PDMAEMA-*b*-PCL-*b*-PDMAEMA Triblock Copolymers for the Encapsulation of Amphotericin B

Ivonne L. Diaz,[1] Claudia Parra,[2] Melva Linarez,[2] and Leon D. Perez[3,4]

Received 12 December 2014; accepted 19 January 2015; published online 11 February 2015

Abstract. The clinical application of amphotericin B (AmB), a broad spectrum antifungal agent, is limited by its poor solubility in aqueous medium and also by its proven renal toxicity. In this work, AmB was encapsulated in micelles obtained from the self-assembly of PDMAEMA-b-PCL-*b*-PDMAEMA triblock copolymers. The amount of encapsulated AmB depended on the copolymer composition, and short blocks of polycaprolactone (PCL) and poly(2-dimethylaminoethyl methacrylate) (PDMAEMA) showed better performance. All the studied formulations exhibited a controlled release of AmB along 150 h. The formulations presented reduced hemotoxicity while maintaining antifungal activities against *Candida albicans*, *Candida krusei*, and *Candida glabrata* comparable with free AmB. A reduction on the hemotoxicity was found to be due to the slow release and subsequent low aggregation achieved with the use of polymer micelle nanocontainers.

KEY WORDS: amphotericin B; antifungal agent; hemotoxicity; micelles.

INTRODUCTION

Amphotericin B (AmB) is a macrolide polyene antifungal agent available for clinical use since its initial FDA approval in 1959. AmB itself is insoluble in aqueous media; conventionally, it is formulated as a colloidal dispersion employing deoxycholate, as a surfactant. The antifungal effect of AmB is related to its amphiphilic character endowed by the presence of a hydrophobic (polyene hydrocarbon chain) and a hydrophilic (poly-hydroxyl chain) region. The hydrophobic interaction of AmB with ergosterol molecules in the fungal cells results in the formation of pores, which facilitate rapid efflux of K^+, inhibition of fungal glycolysis, and subsequent Mg^{+2} efflux. This loss along with a subsequent influx of protons into the fungal cell causes acidification of the fungal interior with precipitation of the cytoplasm and ultimate cell death [1–3].

AmB exhibits good activity against a broad spectrum of clinically relevant fungi. However, its use is hampered by its demonstrated renal toxicity rendering the conventional formulations of AmB unsuitable for clinical use [4]. It has been established that the toxicity associated to AmB is due to the formation of soluble aggregates. Legrand and coworkers pointed out that the toxicity to human erythrocytes is due to the interaction between those aggregates and cholesterol in cell membranes causing K^+ leakage [5].

It has been demonstrated that lipid-based formulations increase the solubility of AmB and decrease its toxic side effects overcoming the disadvantages of conventional formulations while maintaining similar efficacy [6, 7]. The major drawbacks of the lipid-based systems are high dose requirement and high costs.

The use of polymer micelles (PMs) obtained by self-assembly of block copolymers in aqueous media, as nanocontainers for hydrophobic or poorly soluble drugs, has attracted great interest [8–12]. PMs are composed of two separated domains: an inner core and an outer shell. The outer shell controls the micelle solubility and *in vivo* interaction with tissues and cells, while the inner core is responsible for drug loading and stability. The properties of PMs result from their high colloidal stability which is afforded by the presence of hydrophilic segments and their low critical micelle concentration (CMC) compared to low molecular weight surfactants. Some of the advantages of using PMs as drug nanocarriers include their ability to protect the drugs allowing them to maintain their activity, reduce their toxicity and secondary effects during the circulation time, and also permit controlling its concentration in the plasma [13].

The used of PMs to encapsulate AmB has been investigated by other authors, who report that on the encapsulation, the hemotoxicity associated to AmB decreases [14–17]. Block copolymers composed of polycaprolactone (PCL) and poly(2-dimethylaminoethyl methacrylate) (PDMAEMA) evoke great interest for this application due to the outstanding physical and chemical properties of the individual blocks. PCL, a

[1] Departamento de Química, Pontificia Universidad Javeriana, Carrera 7 No. 40-62, Bogotá D.C., Colombia.
[2] Departamento de Microbiología, Pontificia Universidad Javeriana, Carrera 7 No. 40-62, Bogotá D.C., Colombia.
[3] Departamento de Química, Universidad Nacional de Colombia, Carrera 45 No. 26-85, edificio 451 of. 449, Bogotá D.C., Colombia.
[4] To whom correspondence should be addressed. (e-mail: ldperezp@unal.edu.co)

 1530-9932/15/0500-1069/0 © 2015 American Association of Pharmaceutical Scientists

hydrophobic polymer approved by the FDA for biomedical applications, is biocompatible, biodegradable, and highly permeable to drugs and presents high capacity of encapsulating hydrophobic substances [18, 19].

There are numerous reports concerning about the synthesis of block copolymers containing PCL as hydrophobic segment and its application in the fabrication of micelles for drug delivery. PCL is commonly combined with hydrophilic blocks such as polyvinylpyrrolidone, polyethylene glycol, and poly(*N*-isopropylacrylamide), with successful application in the encapsulation of drugs [20–23]. On the other hand, copolymers containing PDMAEMA are biocompatible and exhibit pH responsive behavior, which renders these materials very promising for the design of sensitive drug delivery systems [24–29].

The interaction of PMs with low molecular weight nonpolar drugs is well described in the literature, and it is clearly assumed that the hydrophobic cores of micelles are responsible for their solubilization [30–32]. Some characteristics of AmB such as its high molecular weight and amphiphilic character result in more complex interactions with micelles dispersed in aqueous medium. In this work, micelle nanocontainers obtained from PDMAEMA-*b*-PCL-*b*-PDMAEMA triblock copolymers were used for encapsulating AmB. Additionally, the effect of the composition of the copolymers on properties such as encapsulation efficiency, hemotoxicity, and biological activity was established.

EXPERIMENTAL SECTION

Materials

Poly(ε-caprolactone) diol (M_n=2000 and 10,000 g/mol), pyrene (98%), amphotericin B (80%), sodium dodecyl sulfate (SDS, >99%), and analytical grade solvents such as dichloromethane, tetrahydrofuran (THF), dimethyl sulfoxide, and *N,N*-dimethylformamide were supplied by Sigma-Aldrich and used without any further purification. Dialysis membranes with a molecular weight cutoff of 12 kDa were supplied by Thermo Scientific. The culture media Müeller Hinton agar and Saboraud dextrose agar were purchased from Panreac.

Synthesis of PDMAEMA-*b*-PCL-*b*-PDMAEMA Triblock Copolymers

Triblock copolymers composed of an inner PCL segment and two side PDMAEMA segments (Scheme 1) were synthesized via atom transference radical polymerization according to a protocol early published [33]. The composition and molecular weight dispersity of copolymers obtained at three different polymerization times were estimated using ^{1}HNMR and gel permeation chromatography. CMC was measured at pH 5.0 using pyrene as hydrophobic probe, according to procedures early reported [34, 35]. The composition of the copolymers, molecular weight and dispersity, and CMC values are listed in Table I.

Formation of Micelles

The copolymer micelles were prepared by a nanoprecipitation method [36]. In detail, 20 mg of copolymer sample was dissolved in 2.5 mL of acetone. Then, the solution was dropwise into 5 mL of a buffer solution of pH 5.0 under vigorous stirring. The resulting dispersion was maintained under stirring during 24 h at room temperature to allow acetone evaporation.

Characterization Techniques

The average diameter of micelles was determined by dynamic light scattering (DLS) using a Horiba LB 550 equipment. The measurements were carried out at 23°C in aqueous dilutions of the samples (≈1/20) prepared using deionized water (~18 MΩ cm), in order to avoid particle-particle interactions and multiple scattering effects. Zeta potential was measured using a zeta potential analyzer Malvern Zetasizer Nano ZS. Zeta potential was determined three times for each sample.

For TEM analysis, 2 μL of the diluted samples (0.1 mg/mL) were spilled into a copper grid Formvar® coated and dried at room temperature during 24 h, and the images were obtained in a Jeol 1400 plus microscope.

Preparation of AmB-Loaded Micelles

A typical protocol for the preparation of AmB-loaded micelles was as follows: 2 mg of AmB was dissolved in 2 mL of methanol and slowly dropped (10 μL/min) into 10 mL of a micelle solution at pH 5.0 containing 40 mg/mL of the corresponding copolymer. The resulting solution was gently stirred during 1 h under reduced pressure to eliminate methanol residuals. Finally, the dispersion was centrifuged at 10,000 rpm to eliminate the nonencapsulated AmB and lyophilized for its posterior use.

The amount of AmB encapsulated in the PM was determined by UV-Vis spectroscopy using a Varian Cary 100. The quantification was performed as follows: aliquots of 1 mL of encapsulated AmB aqueous dispersions were mixed with an equal volume of dimethylformamide (DMF) and analyzed by UV-Vis, and the quantification was performed using a calibration curve obtained from the absorbance at 411 nm, prepared by direct dilution of AmB in a 50:50 (vol/vol) water/DMF mixture.

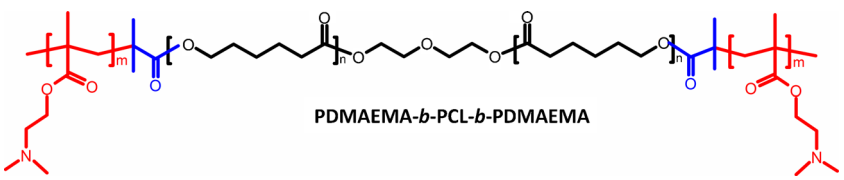

Scheme 1. Structure of PDMAEMA-*b*-PCL-*b*-PDMAEMA amphiphilic triblock copolymers

Table I. Composition, Molecular Weight Distribution, and Critical Micelle Concentration of Triblock Copolymer PDMAEMA-*b*-PCL-*b*-PDMAEMA Samples

Sample	Average composition	M_n (kDa)	M_w/M_n	CMC (mg/L)
P2D1	$(DMAEMA)_{11}$-$(CL)_{17}$-$(DMAEMA)_{11}$	5.4	1.69	4.9
P2D2	$(DMAEMA)_{19}$-$(CL)_{17}$-$(DMAEMA)_{19}$	7.9	1.09	6.8
P2D3	$(DMAEMA)_{28}$-$(CL)_{17}$-$(DMAEMA)_{28}$	10.7	1.57	7.4
P10D1	$(DMAEMA)_{28}$-$(CL)_{88}$-$(DMAEMA)_{28}$	18.8	1.17	0.86
P10D2	$(DMAEMA)_{39}$-$(CL)_{88}$-$(DMAEMA)_{39}$	22.3	1.09	1.0
P10D3	$(DMAEMA)_{61}$-$(CL)_{88}$-$(DMAEMA)_{61}$	29.2	1.15	1.0

CMC critical micelle concentration

The loading efficiency (DLE%) as well as the drug content (DLC) was estimated using equations proposed by Zhang *et al.* [29] as follows:

$$\text{DLC\%} = \frac{\text{amount of AmB in PMs}}{\text{amount of AmB} + \text{PMs}} \quad (1)$$

$$\text{DLE\%} = \frac{\text{amount of AmB in PMs}}{\text{amount of AmB used for PM preparation}} \quad (2)$$

In Vitro Release of AmB from Polymeric Micelles

In vitro release of AmB from AmB-loaded PMs was studied based on a protocol published by Wang *et al.* [37]. Briefly, 4.0 mL of the AmB-loaded micelles dispersed in PBS pH 7.4 (4 mg of the formulation/1 mL of buffer) were transferred to a dialysis bag (MWCO 12 kDa) and placed in 50.0 mL of two different media at 37°C: (1) sink medium—a solution of sodium dodecyl sulfate 1 wt% in PBS, pH 7.4; and (2) nonsink medium—PBS, pH 7.4. The temperature was maintained constant using a thermostatic bath. At selected time intervals, 2 mL of the release medium (outside the dialysis bag) was diluted with equal volume of DMSO and monitored by UV-Vis, and the volume of the releasing medium was maintained constant by the addition of fresh solution. The concentration of AmB was determined based on the absorbance intensity at 411 nm using a standard calibration curve obtained from solutions with different concentrations of AmB in PBS/DMSO (1:1).

In Vitro Hemolytic Activity

Human blood was diluted with PBS pH 7.4 in a volume ratio of 1:4 and centrifuged at 2000 rpm, and the supernatant and buffy coat were removed. Red blood cells (RBCs) were diluted in PBS to obtain absorbance values between 0.4 and 0.5. In an initial experiment, dispersions of RBCs were charged with five different concentrations (5, 10, 15, 20, and 25 ppm) of free and encapsulated AmB (the volume was adjusted to obtain an equal concentration of RBCs) and were incubated at 37°C during 30 min and placed in ice afterward to stop hemolysis. In a second experiment, dispersions of RBCs with 10 ppm of free and encapsulated AmB were incubated during 24 h, and the hemolysis was monitored at regular time intervals.

The unlysed RBCs were removed by centrifugation at 14,000 rpm during 20 s, and the supernatants were analyzed by UV-Vis at 576 nm. Free AmB in PBS (20 ppm) was used as a positive control while the negative control was prepared with no AmB added.

The hemolysis percentage was determined using the following equation [38]:

$$\text{Hemolysis}\,(\%) = \frac{\text{Abs} - \text{Abs}_0}{\text{Abs}_{100} - \text{Abs}_0} \times 100 \quad (3)$$

where Abs corresponds to the absorbance obtained for each sample, and Abs_0 and Abs_{100} correspond to the absorbance of the negative and positive control, respectively.

In Vitro Antifungal Activity

The antifungal activity of AmB-loaded micelles against three different yeast strains (*Candida albicans*, *Candida krusei*, and *Candida glabrata*) was assessed by agar diffusion assay according to procedures previously reported [39–41]. Prior to the analysis, yeast isolates were cultured on a Sabouraud dextrose agar at 30°C for 24 h to ensure viability and absence of contamination. Then, the yeast isolates were suspended in a sterile saline solution to obtain an optical density of 0.5 McFarland units, which corresponds to a range of 11×10^6–5×10^6 CFU/mL. Petri dishes containing Müller Hilton agar were inoculated using a brush previously soaked with yeast suspensions. Eight assay cylinders (diameter 5 mm) were placed equidistance apart in yeast-coated disks. The cylinders were loaded with 50 μL of a reference solution composed of AmB dissolved in a mixture of PBS/DMSO and AmB-micelle formulations dissolved in PBS. Finally, the disks were incubated at 37°C during 24 h, and the inhibition halos were measured.

RESULTS AND DISCUSSION

Micelle Characterization

Micelles are colloidal systems obtained by self-assembly of amphiphilic molecules in a solvent that solubilizes one of the blocks. In the case of aqueous micelles, one of the blocks must be hydrophilic, providing the micelles affinity for aqueous medium. The stability of the micelles can be attributed to two main aspects: thermodynamic stability and kinetic

stability which mainly depend on the composition and molecular weight of the copolymer.

Conventionally, critical micelle concentration, besides serving as a strong evidence of the self-association of block copolymers, also provides information about the stability of micelles. Copolymers with high CMC values seem to be unsuitable because the formed micelles may be dissociated after being administered into the body because of the dilution effect. From this point of view, a low CMC indicates that the nanocontainers are more stable against dilution and, therefore, could provide a controlled release of the drug. However, low CMC values are achieved for bulky and stiff hydrophobic blocks and when the polymer chains forming the micelle core interact strongly. Those conditions reduce the rate of micelle disassembly affecting both the release of the drug and their elimination by the kidney [42].

In the case of PDMAEMA-*b*-PCL-*b*-PDMAEMA (Table I), the CMC of the copolymers depends on their composition, being mainly affected by the length of the hydrophobic block. Thus, copolymers containing a PCL segment of 10 kDa presented the lowest CMC below 1 mg/L. These results agree with other authors who pointed out that long hydrophobic blocks push the CMC to low values [20, 29, 43, 44]. On the other hand, CMC is less sensitive to the length of PDMAEMA.

The morphology and size distribution of the copolymer micelles were investigated by TEM and DLS, respectively. Diameter distribution plots of micelles measured at pH 5.0 are depicted in Fig. 1a, b, and the corresponding average values are listed in Table II. It is observed that the micelles exhibit a monomodal distribution centered below 100 nm. The size of the micelles is mainly affected by the molecular weight of the hydrophobic PCL segment, and the smaller diameter corresponds to the set of copolymers obtained from PCL of 10 kDa. According to the data in Table II, in all the compositions, the ζ potential value was larger +21 mV, which indicates that the micellar dispersions are positively charged and also present colloidal stability. TEM images presented in Fig. 1c, d indicate that the micelles are spherical and exhibit a core-shell morphology.

Amphotericin B Encapsulation

The encapsulation of AmB in micelles obtained by the self-assembly of PDMAEMA-*b*-PCL-*b*-PDMAEMA triblock copolymers with different compositions was carried out by partition of AmB in preformed micelles. The DLE and the AmB content (DLC) determined by Eqs. 1 and 2, respectively, are summarized in Table III. According to these values, it is deduced that both DLE and DLC depend on the composition of the copolymers. Micelles containing PCL of 2 kDa and short PDMAEMA segments yield more favorable values.

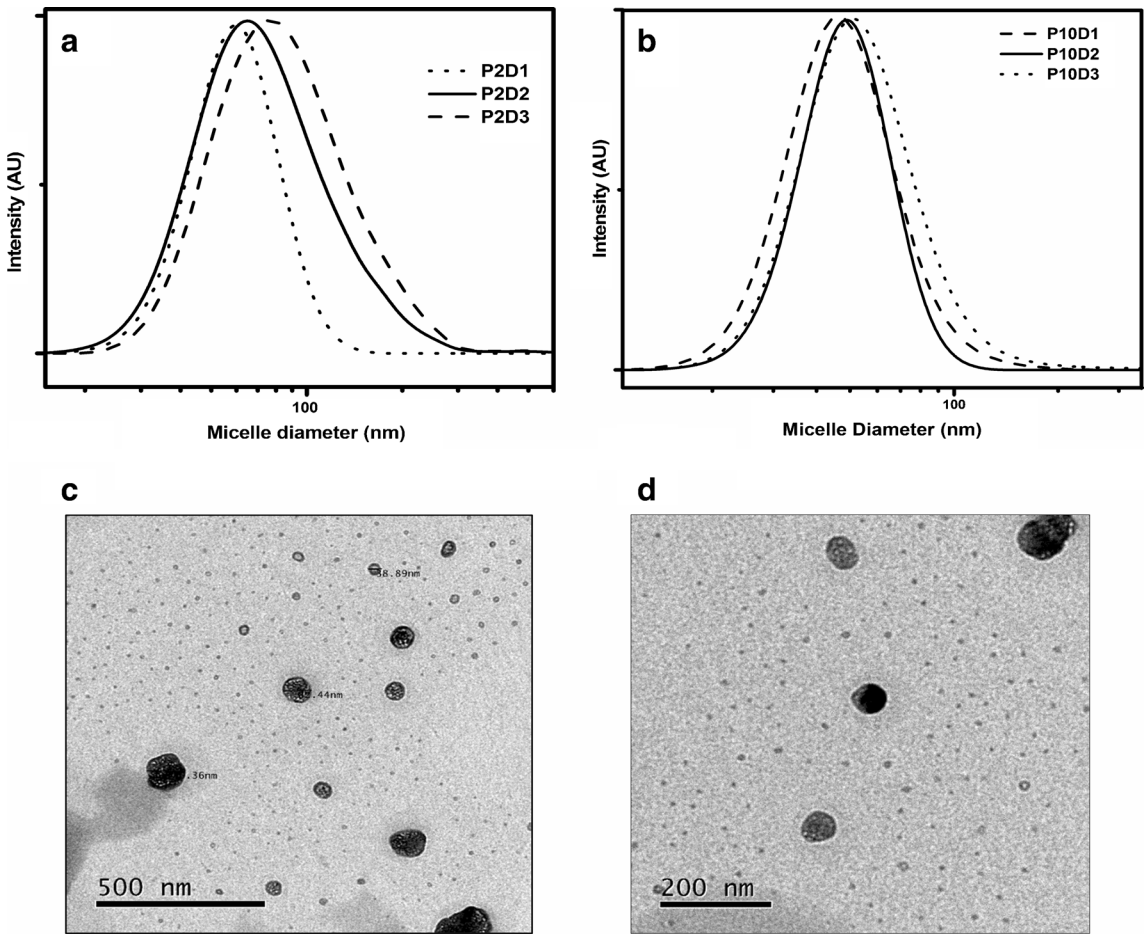

Fig. 1. Particle size distribution of micelles at pH 5.0 for the set of samples obtained from PCL of **a** 2 and **b** 10 kDa. TEM images of the micelles obtained from representative samples: **c** P2D2 and **d** P10D2 supported on a Formvar® coated copper grid

Table II. Characterization of the Micelles Obtained by Self-Assembly of PDMAEMA-*b*-PCL-*b*-PDMAEMA Triblock Copolymers in Aqueous Medium at pH 5.0

Sample	Micelle diameter (nm)	ζ potential (mV)
P2D1	57±13	22±13
P2D2	82±18	25±19
P2D3	85±26	27±16
P10D1	46±17	41±10
P10D2	47±28	30±11
P10D3	54±27	37±14

The extent of drug incorporation in PMs by partition is affected by the solubility of the drug in water and also by the chemical characteristics of the copolymer, which in turn determines the affinity of the drug for the micelle core and the micelle dynamics. The drug affinity for a micelle core can be described in terms of the Flory-Huggins interaction parameter defined as follows [30]:

$$\chi_{sp} = \frac{(\delta_s - \delta_p)^2 V_s}{RT} \quad (4)$$

where δ_s and δ_p are the Scatchard-Hildebrand solubility parameter of the solute and the core-forming polymer, respectively, V_s is the molar volume of the solute, R is the gas constant, and T is the temperature.

However, in the case of AmB, the scenario is more complex. The literature describes that when AmB is dispersed in an aqueous solution, three different states exist: as monomeric units, soluble aggregates, and poorly soluble superaggregates. Assuming that the Flory-Huggins interaction parameter properly describes its solubility in PCL forming cores, the high volume of AmB unimers and aggregates increases the magnitude of this parameter envisaging poor interaction. On the other hand, the incorporation of AmB into the micelle cores is sterically not favorable. This effect notoriously impacts the encapsulation efficiency.

Besides the chemical affinity of AmB for micelle cores, its encapsulation is also affected by the micelle dynamics, which is less favorable for the copolymer containing the largest hydrophobic segment. On the other hand, a shorter hydrophilic shell could reduce the energy barrier required to transfer AmB unimers and aggregates from the aqueous medium to the hydrophobic core of the micelles [43].

Table III. Characterization of the Formulations, AmB Loading Efficiency, and Content (n=3)

Sample	Loading efficiency (%)	AmB content (%)	Aggregation state AI/AIV
P10D1	47±2	2.4±0.1	3.4
P10D2	46±1	2.3±0.1	2.7
P10D3	45±2	2.3±0.1	2.2
P2D1	82±5	4.1±0.3	4.4
P2D2	68±5	3.4±0.2	4.2
P2D3	57±5	2.9±0.2	3.7

The ratio of AmB dissolved in DMSO was 0.29
AmB amphotericin B

UV-Vis spectra of AmB dissolved in DMSO and PBS and encapsulated in micelles obtained from P2D2 and P10D2 are shown in Fig. 2. The spectrum of AmB in PBS, where it is highly aggregated, presents a strong absorption at 332 nm. Whereas in DMSO, where it is in the monomeric form, the spectra show four absorptions centered at 350, 370, 388, and 415 nm. The marked difference between the spectra of AmB forming aggregates and AmB unimers provides evidence that the absorption of AmB in the UV-Vis region is sensitive to its aggregation state. Hence, the ratio of absorbance at 332 nm (I) (aggregate form) to absorbance at 415 nm (IV) (main absorption of the monomeric form) allows a qualitative assessment of the aggregation state of AmB. This ratio was estimated for each formulation, and the values are listed in Table III. The results indicate that as the amount of AmB encapsulated in the micelles increases, AmB is more aggregated. It corroborates that the encapsulation of this substance proceeds through the incorporation of aggregates in the micelles, and this process seems to be more favorable for larger micelles obtained from copolymers containing PCL of 2 kDa.

From Fig. 2, it is observed that AmB is dissolved in PBS, and AmB-P10D2 is absorbed around 232 nm, while AmB-P2D2 is absorbed at 223 nm. Similar blueshifting of the absorption due to the AmB aggregates has been reported in the presence of deoxycholate, and it has been attributed to the interaction of deoxycholate with AmB aggregates that cause the monomers to move closer to each other [45, 46]. It allows inferring that micelles obtained from PCL of 2 kDa present a stronger interaction with AmB aggregates than micelles composed of PCL of 10 kDa.

In Vitro Release of AmB

Figure 3a, b presents the release profiles of AmB from AmB-loaded micelles under sink conditions achieved using 1% SDS in the release medium; according to Jain and Kumar, the solubility of AmB in this solution is 224.7 μg/mL [47]. The plots show that these formulations exhibit a controlled release

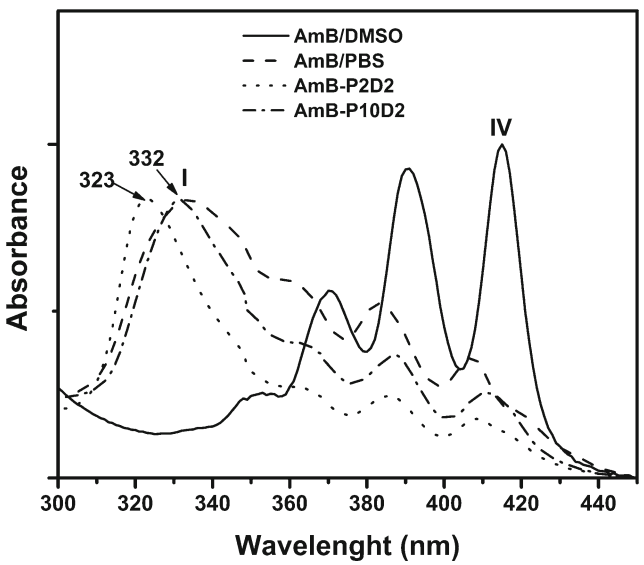

Fig. 2. UV-Vis spectrum of AmB dissolved in PBS and DMSO, and AmB encapsulated in micelles obtained from representative copolymer samples P2D2 and P10D2

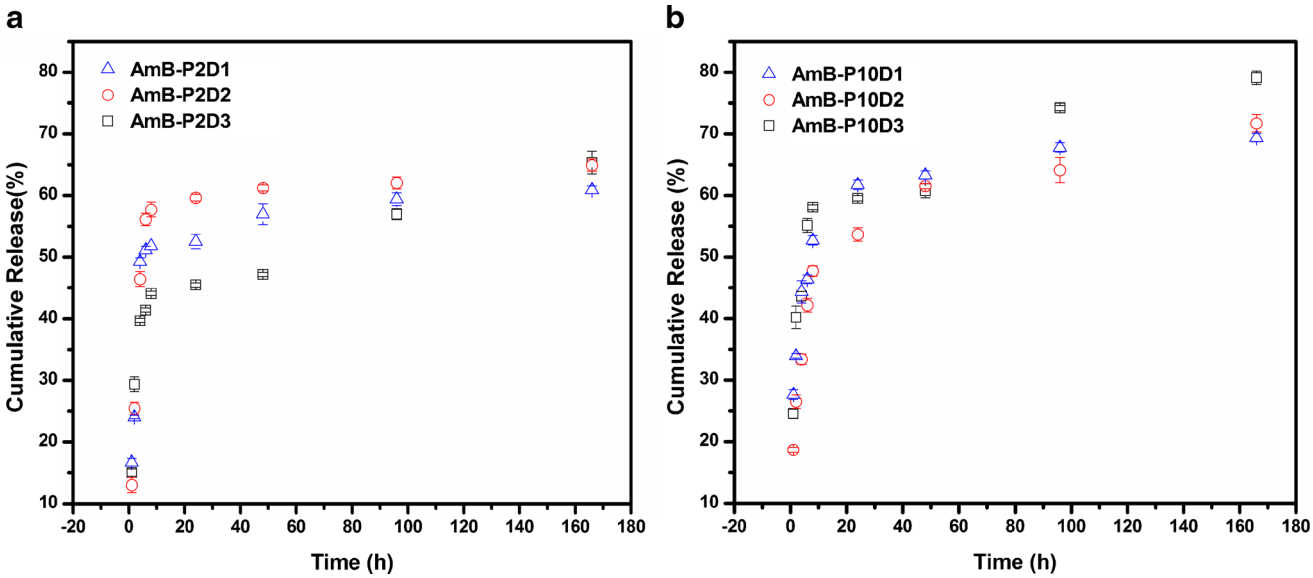

Fig. 3. Release profiles of AmB under sink conditions achieved by the incorporation of SDS in the release medium from AmB encapsulated in micelles obtained from copolymers containing a segment of PCL of **a** 2 and **b** 10 kDa

along 150 h. For each sample, the release profiles exhibit two different regions: an initial burst during the first 24 h and then a minor release rate. After 150 h, formulations obtained from micelles with an inner PCL segment of 2 kDa released around 60% of AmB, while the corresponding cumulative release for formulations containing PCL of 10 kDa was larger than 70%.

In another experiment, using PBS as the release medium, the concentration of AmB was monitored along 150 h. Figure 4a, b reveals that formulations obtained from PCL of 2 kDa showed a small initial release of AmB, and also the equilibrium concentration of AmB measured after 150 h was smaller than 0.3 ppm. On the other hand, the set of PM that contains PCL of 10 kDa showed a faster release; after 30 min, the concentration of AmB was larger than 0.3 ppm; and the concentration at 150 h was in the range of 0.6 to 1.2 ppm, depending on the length of the PDMAEMA segment.

Diffusion and dissolution of micelles are the main mechanisms that account for the release of hydrophobic substances from PM [48]. Due to the fact that encapsulated AmB is forming aggregates, diffusional processes are less favorable. Instead, the micelle dynamics (unimers exchange) could be the process responsible for releasing AmB.

The results indicate that copolymers composed by PCL of 2 kDa are more suitable for the fabrication of nanocontainers for AmB. They encapsulate a larger amount of AmB, interact stronger with the aggregates as deduced from the hypsochromic shift in the UV-Spectra, and also present low equilibrium concentration of AmB under nonsink conditions. The difference between both sets of copolymers is related to the way how the micelles interact with AmB.

For micelles containing PCL of 10 kDa, the dynamic phenomena responsible for the encapsulation of the AmB

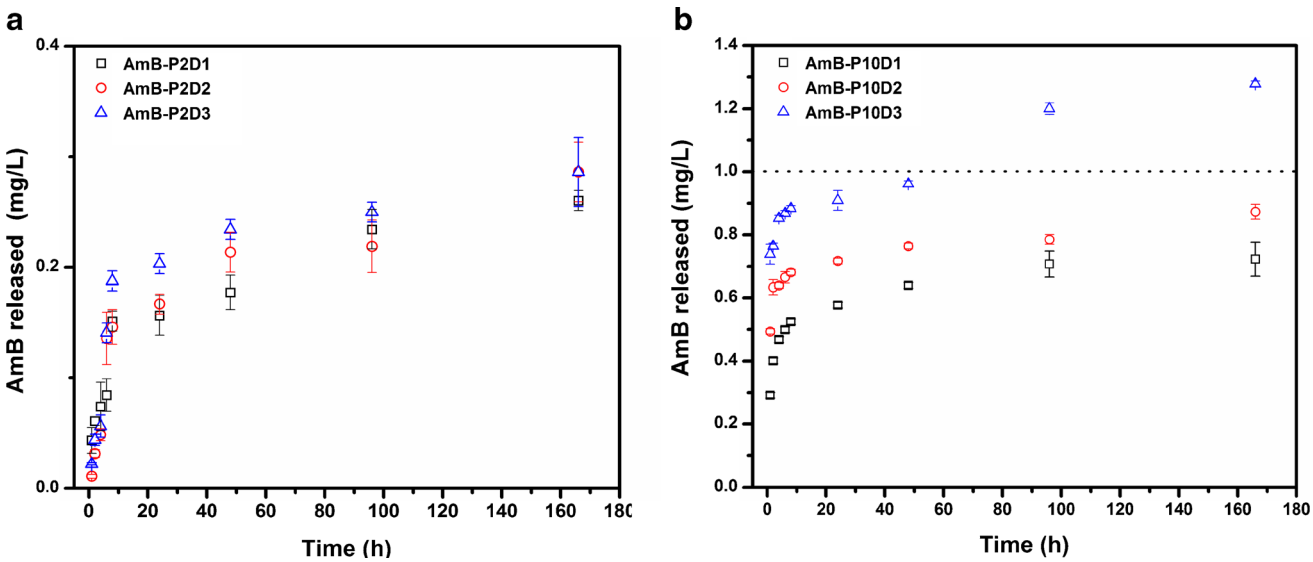

Fig. 4. Effect of PDMAEMA block length on the release profiles in formulations obtained from PDMAEMA-*b*-PCL-*b*-PDMAEMA with different lengths of PCL: **a** 2 and **b** 10 kDa (n=3)

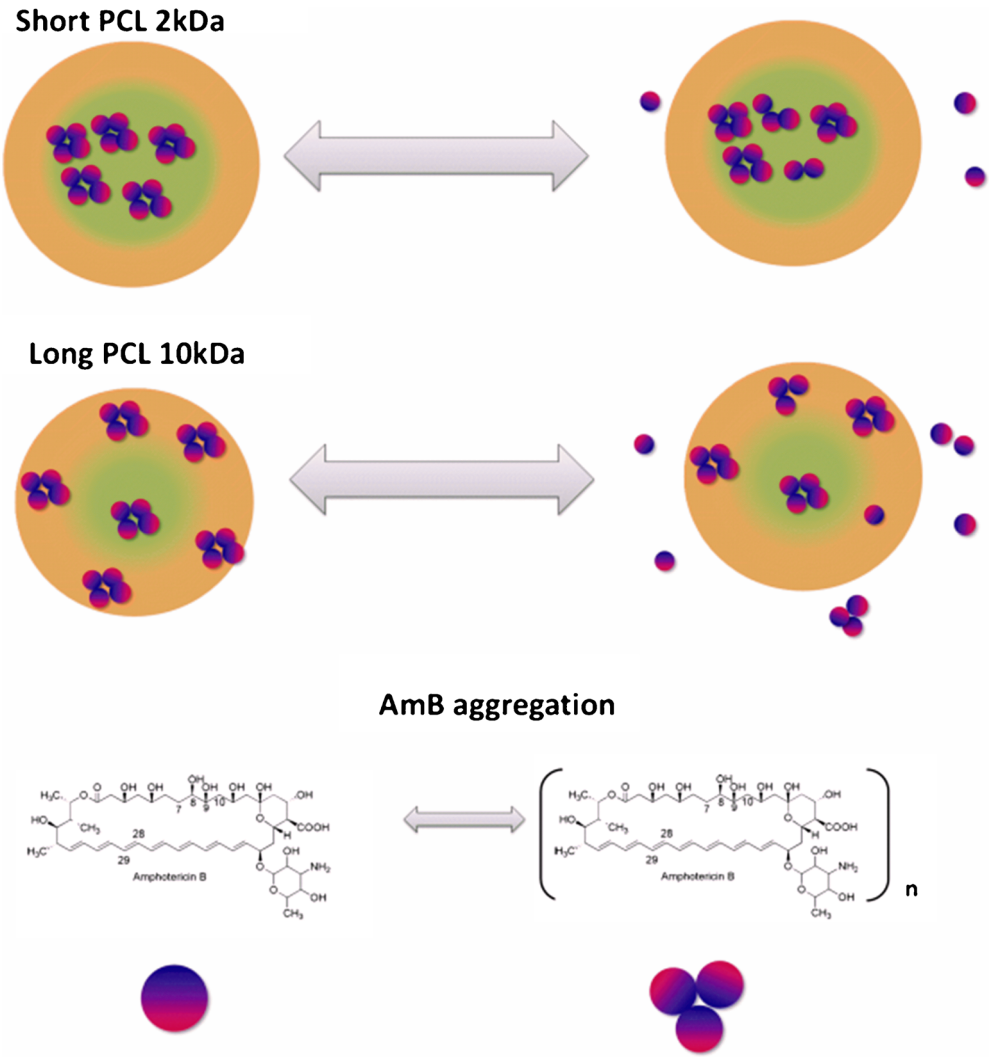

Scheme 2. Encapsulation of AmB in micelles obtained from copolymers containing PCL of 2 and 10 kDa

are less favorable, as well as their smaller and denser micellar core. Likely, a significant fraction of encapsulated AmB is located at the interfacial region (PDMAEMA-PCL), which is enabled by its amphiphilic nature, as schematically shown in Scheme 2. Specific interactions between AmB aggregates and unimers and PDMAEMA are afforded by the presence of polar groups such as hydroxyl and amine.

In Vitro Hemolytic Activity

In order to assess the *in vitro* toxicity of encapsulated AmB against human erythrocytes, hemolysis induced by different concentrations of free and encapsulated AmB was studied. The hemolysis of nonencapsulated AmB (denoted as free AmB) at 5, 10, and 15 ppm were 23, 28, and 43%, respectively, and at concentrations of 20 and 25 ppm, the hemolysis was 100%. From Fig. 5, it is deduced that the encapsulation reduces the hemolytic activity; even at the highest concentration of 25 ppm, the hemolysis percentage was kept low in the range of 2.7 to 28.4%. The empty micelles (data no shown) did not present hemolytic activity.

At all the concentrations of AmB, the formulations obtained from copolymers containing PCL of 2 kDa presented

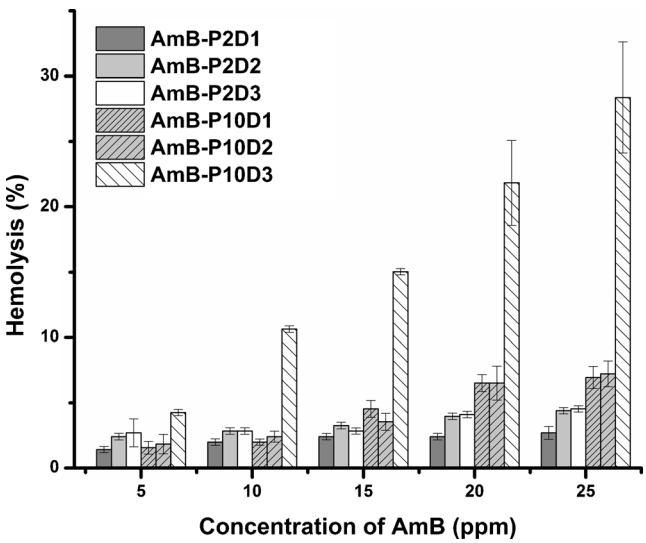

Fig. 5. Effect of the composition of PDMAEMA-*b*-PCL-*b*-PDMAEMA and concentration of AmB on the hemolytic activity (n=3)

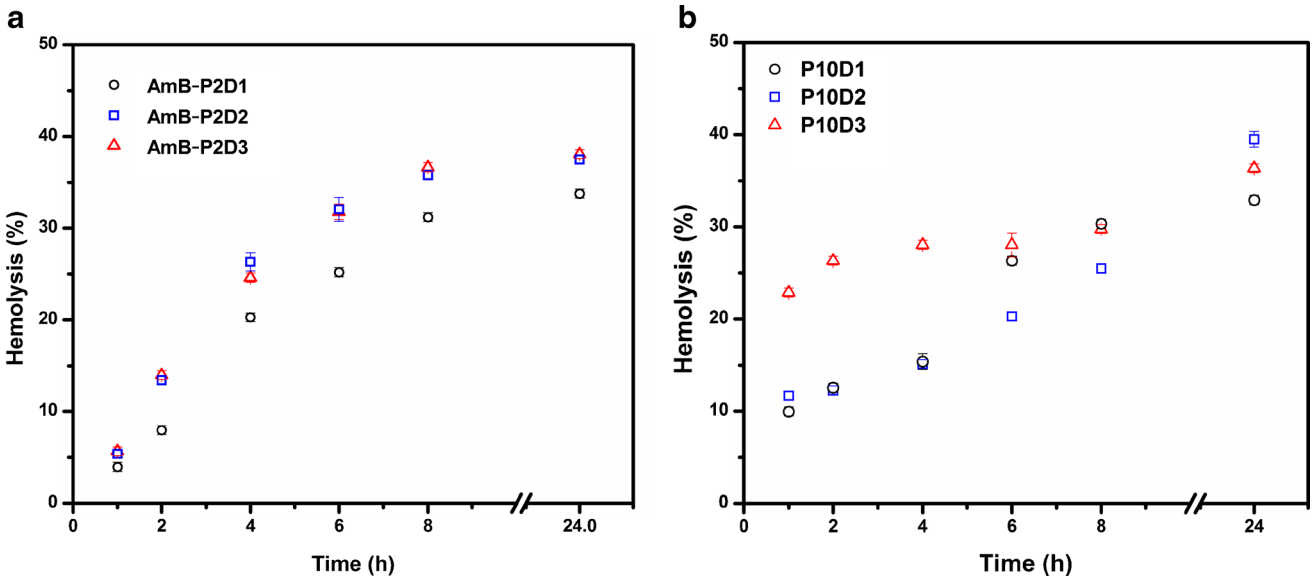

Fig. 6. Hemolytic activity of AmB encapsulated in micelles obtained from PDMAEMA-*b*-PCL-*b*-PDMAEMA with different lengths of PCL: **a** 2 and **b** 10 kDa (n=3)

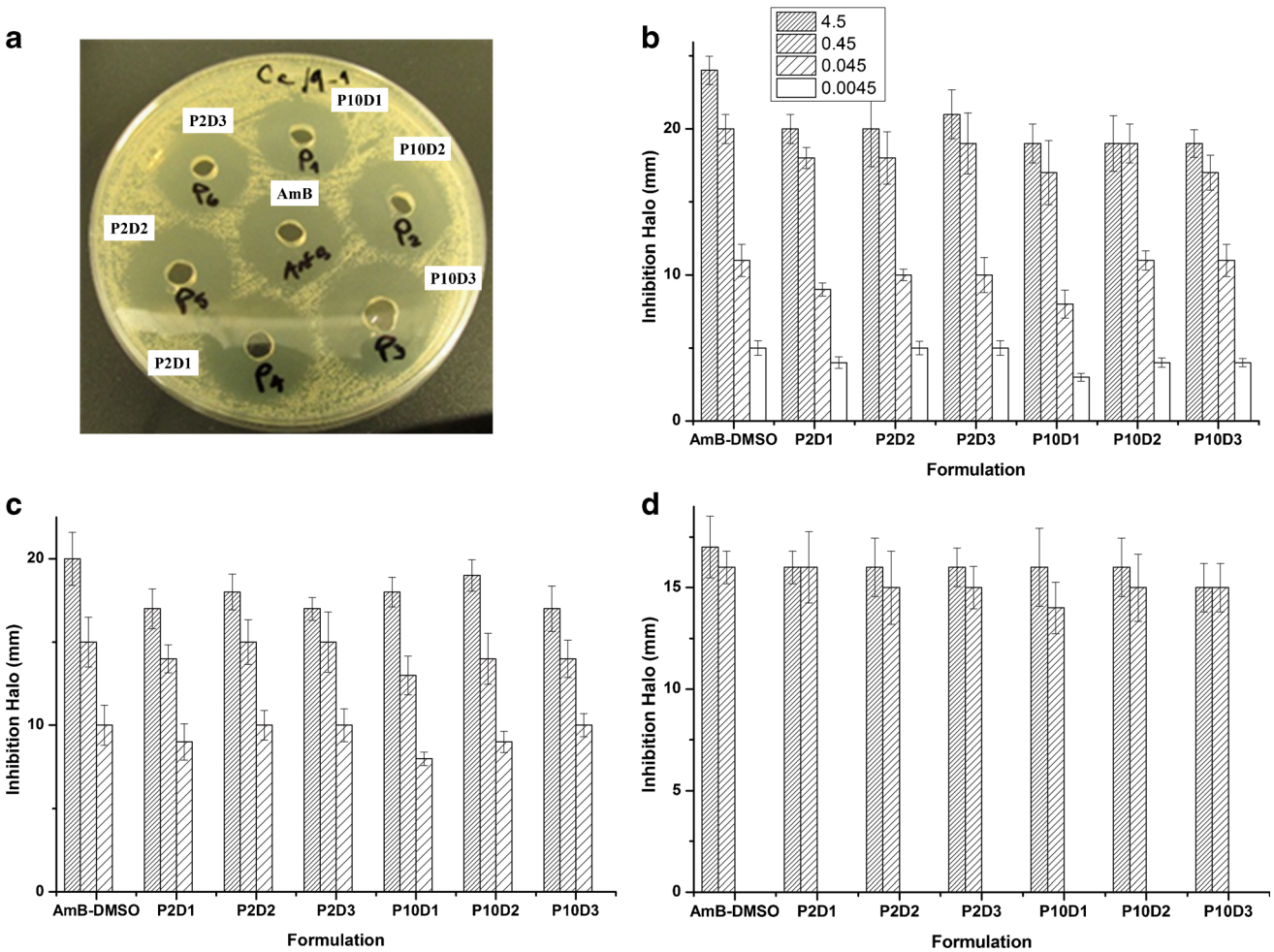

Fig. 7. **a** Representative picture showing the inhibition halos observed for *C. albicans* using AmB dissolved in DMSO and encapsulated in micelles obtained from the evaluated copolymer; the final concentration of AmB in each cylinder was 9 ppm. Inhibition halos of **b** *C. albicans*, **c** *C. krusei*, and **d** *C. glabrata* obtained at four different concentrations of free and encapsulated AmB

the lowest hemolytic activity showing a good correlation with the release profiles obtained under nonsink conditions (without SDS). A lower concentration of AmB in the release medium corresponds to a lower concentration of aggregates which are responsible for the hemotoxicity. Previous studies indicate that AmB aggregates can interact with cholesterol units contained in the erythrocytes membranes, causing the formation of pores and changes in the electrolyte balance[5, 49].

To further confirm the reduced toxicity of AmB on the encapsulation, hemolysis experiments were conducted along 24 h with a fixed concentration of AmB (10 ppm); the hemolysis was monitored regularly, as shown in Fig. 6. The set of copolymers composed of PCL of 2 kDa presented lowest initial hemolysis. After 24 h, the hemolysis was lower than 40%, which indicates that micelles obtained from PDMAEMA-*b*-PCL-*b*-PDMAEMA reduce the hemotoxicity of AmB.

In Vitro Antifungal Activity

The antifungal activity of AmB-loaded micelles against three different strains (*C. albicans*, *C. krusei*, and *C. glabrata*) was determined by agar diffusion halo assay. Previous researches have demonstrated that measurement of inhibition halos is a reliable methodology to detect sensitivity of yeast strains to AmB formulations [50, 51]. Figure 7a shows a representative picture of the inhibit halos on *C. albicans* obtained for free AmB and the formulations based on polymer micelles using a fixed concentration of AmB of 9 ppm. The inhibition halos obtained for the tested strains using different concentrations of free and encapsulated AmB are shown in Fig. 7b–d. According to the results, the encapsulated AmB exhibits an antifungal activity against the tested strains tested (*C. albicans*, *C. krusei*, and *C. glabrata*) comparable to AmB dissolved in DMSO. On the other hand, the composition of the copolymer showed no effect on the inhibition halos.

CONCLUSIONS

Micelles composed of PDMAEMA-*b*-PCL-*b*-PDMAEMA were used as nanocontainers for the encapsulation and controlled release of AmB. The performance of micelles showed to depend on the composition of copolymers and their polymerization degree. The encapsulation of AmB was favored for copolymers with the shortest PCL and PDMAEMA blocks. On encapsulation, the hemotoxicity was significantly reduced, while its antifungal activity was comparable with nonencapsulated AmB.

ACKNOWLEDGEMENTS

The authors thank to the Pontificia Universidad Javeriana for the financial support throught the grant number 5620.

REFERENCES

1. Gallis HA, Drew RH, Pickard WW. Amphotericin B: 30 years of clinical experience. Rev Infect Dis. 1990;12:308–29.
2. Hamill R. Amphotericin B formulations: a comparative review of efficacy and toxicity. Drugs. 2013;73:919–34.
3. Groll A, Walsh T. Uncommon opportunistic fungi: new nosocomial threats. Clin Microbiol Infect. 2001;7:8–24.
4. Deray G. Amphotericin B, nephrotoxicity. J Antimicrob Chemother. 2002;49:37–41.
5. Legrand P, Romero EA, Cohen BE, Bolard J. Effects of aggregation and solvent on the toxicity of amphotericin B to human erythrocytes. Antimicrob Agents Chemother. 1992;36:2518–22.
6. Ringdén O, Meunier F, Tollemar J, Ricci P, Tura S, Kuse E, et al. Efficacy of amphotericin B encapsulated in liposomes (AmBisome) in the treatment of invasive fungal infections in immunocompromised patients. J Antimicrob Chemother. 1991;28:73–82.
7. Walsh TJ, Finberg RW, Arndt C, Hiemenz J, Schwartz C, Bodensteiner D, et al. Liposomal amphotericin B for empirical therapy in patients with persistent fever and neutropenia. N Engl J Med. 1999;340:764–71.
8. Alexandridis P, Lindman B. Amphiphilic block copolymers: self-assembly and applications. Amsterdam: Elsevier; 2000.
9. Torchilin VP. Structure and design of polymeric surfactant-based drug delivery systems. J Control Release. 2001;73:137–72.
10. Loh XJ, Wu Y-L, Joseph Seow WT, Irzuan Norimzan MN, Zhang Z-X, Xu F-J, et al. Micellization and phase transition behavior of thermosensitive poly (*N*-isopropylacrylamide)–poly (ε-caprolactone)–poly (*N*-isopropylacrylamide) triblock copolymers. Polymer. 2008;49:5084–94.
11. Cabral H, Kataoka K. Progress of drug-loaded polymeric micelles into clinical studies. J Control Release. 2014;190:465–76.
12. Pippa N, Mariaki M, Pispas S, Demetzos C. Preparation, development and in vitro release evaluation of amphotericin B-loaded amphiphilic block copolymer vectors. Int J Pharm. 2014;473:80–6.
13. Yoon H-J, Jang W-D. Polymeric supramolecular systems for drug delivery. J Mater Chem. 2010;20:211–22.
14. Falamarzian A, Lavasanifar A. Chemical modification of hydrophobic block in poly(ethylene oxide) poly(caprolactone) based nanocarriers: effect on the solubilization and hemolytic activity of amphotericin B. Macromol Biosci. 2010;10:648–56.
15. Adams ML, Andes DR, Kwon GS. Amphotericin B encapsulated in micelles based on poly(ethylene oxide)-block-poly(L-amino acid) derivatives exerts reduced in vitro hemolysis but maintains potent in vivo antifungal activity. Biomacromolecules. 2003;4:750–7.
16. Yang ZL, Yang KW, Li XR, Liu Y. Preparation and in vitro release kinetics of amphotericin B-loaded poly (ethyleneglycol)-poly (dl-lactide) block copolymer micelles. Chin Pharm J. 2007;42:519–23.
17. Adams ML, Kwon GS. Relative aggregation state and hemolytic activity of amphotericin B encapsulated by poly(ethylene oxide)-block–poly(N-hexyl-l-aspartamide)-acyl conjugate micelles: effects of acyl chain length. J Control Release. 2003;87:23–32.
18. Sinha V, Bansal K, Kaushik R, Kumria R, Trehan A. Poly-ϵ-caprolactone microspheres and nanospheres: an overview. Int J Pharm. 2004;278:1–23.
19. Nair LS, Laurencin CT. Biodegradable polymers as biomaterials. Prog Polym Sci. 2007;32:762–98.
20. Gaucher G, Dufresne M-H, Sant VP, Kang N, Maysinger D, Leroux J-C. Block copolymer micelles: preparation, characterization and application in drug delivery. J Control Release. 2005;109:169–88.
21. Burt HM, Zhang X, Toleikis P, Embree L, Hunter WL. Development of copolymers of poly (D, L-lactide) and methoxypolyethylene glycol as micellar carriers of paclitaxel. Colloids Surf B: Biointerfaces. 1999;16:161–71.
22. Shuai X, Ai H, Nasongkla N, Kim S, Gao J. Micellar carriers based on block copolymers of poly (ε-caprolactone) and poly (ethylene glycol) for doxorubicin delivery. J Control Release. 2004;98:415–26.
23. Aliabadi HM, Elhasi S, Mahmud A, Gulamhusein R, Mahdipoor P, Lavasanifar A. Encapsulation of hydrophobic drugs in polymeric micelles through co-solvent evaporation: the effect of solvent composition on micellar properties and drug loading. Int J Pharm. 2007;329:158–65.
24. Xu F, Neoh K, Kang E. Bioactive surfaces and biomaterials via atom transfer radical polymerization. Prog Polym Sci. 2009;34:719–61.
25. Qian X, Long L, Shi Z, Liu C, Qiu M, Sheng J, et al. Star-branched amphiphilic PLA-b-PDMAEMA copolymers for co-delivery of miR-21 inhibitor and doxorubicin to treat glioma. Biomaterials. 2014;35:2322–35.

26. Lee AS, Gast AP, Bütün V, Armes SP. Characterizing the structure of pH dependent polyelectrolyte block copolymer micelles. Macromolecules. 1999;32:4302–10.
27. Baines F, Billingham N, Armes S. Synthesis and solution properties of water-soluble hydrophilic-hydrophobic block copolymers. Macromolecules. 1996;29:3416–20.
28. Liu S, Weaver JV, Tang Y, Billingham NC, Armes SP, Tribe K. Synthesis of shell cross-linked micelles with pH-responsive cores using ABC triblock copolymers. Macromolecules. 2002;35:6121–31.
29. Zhang W, He J, Liu Z, Ni P, Zhu X. Biocompatible and pH-responsive triblock copolymer mPEG-b-PCL-b-PDMAEMA: synthesis, self-assembly, and application. J Polym Sci A Polym Chem. 2010;48:1079–91.
30. Lavasanifar A, Samuel J, Kwon GS. Poly(ethylene oxide)-block-poly(l-amino acid) micelles for drug delivery. Adv Drug Deliv Rev. 2002;54:169–90.
31. Lebouille JJL, Vleugels LW, Dias A, Leermakers FM, Cohen Stuart M, Tuinier R. Controlled block copolymer micelle formation for encapsulation of hydrophobic ingredients. Eur Phys J E. 2013;36:1–12.
32. McLaughlin CK, Logie J, Shoichet MS. Core and corona modifications for the design of polymeric micelle drug-delivery systems. Isr J Chem. 2013;53:670–9.
33. Diaz I, Perez L. Synthesis and micellization properties of triblock copolymers PDMAEMA-b-PCL-b-PDMAEMA and their applications in the fabrication of amphotericin B-loaded nanocontainers. Colloid Polym Sci. 2014;1–11.
34. Maiti S, Chatterji PR, Nisha C, Manorama S, Aswal VK, Goyal PS. Aggregation and polymerization of PEG-based macromonomers with methacryloyl group as the only hydrophobic segment. J Colloid Interface Sci. 2001;240:630–5.
35. Shim WS, Kim SW, Choi EK, Park HJ, Kim JS, Lee DS. Novel pH sensitive block copolymer micelles for solvent free drug loading. Macromol Biosci. 2006;6:179–86.
36. Rao JP, Geckeler KE. Polymer nanoparticles: preparation techniques and size-control parameters. Prog Polym Sci. 2011;36:887–913.
37. Wang C-H, Wang W-T, Hsiue G-H. Development of polyion complex micelles for encapsulating and delivering amphotericin B. Biomaterials. 2009;30:3352–8.
38. Lavasanifar A, Samuel J, Sattari S, Kwon GS. Block copolymer micelles for the encapsulation and delivery of amphotericin B. Pharm Res. 2002;19:418–22.
39. Rojas J, García A, López A. Evaluación de dos metodologías para determinar la actividad antimicrobiana de plantas medicinales. Bol Latinoam Caribe Plant Med Aromat. 2005;4:28–32.
40. Luján MC, Pérez Corral C. Cribado para evaluar actividad antibacteriana y antimicótica en plantas utilizadas en medicina popular de Argentina. Rev Cuba Farm 2008;42
41. Fittler A, Kocsis B, Gerlinger I, Botz L. Optimization of bioassay method for the quantitative microbiological determination of amphotericin B. Mycoses. 2010;53:57–61.
42. Allen C, Maysinger D, Eisenberg A. Nano-engineering block copolymer aggregates for drug delivery. Colloids Surf B: Biointerfaces. 1999;16:3–27.
43. Shim YH, Lee HJ, Dubois P, Chung CW, Jeong YI. Amphotericin B aggregation inhibition with novel nanoparticles prepared with poly (ε-caprolactone)/poly (N, N-dimethylamino-2-ethyl methacrylate) diblock copolymer. J Microbiol Biotechnol. 2011;21:28–36.
44. Mok MM, Thiagarajan R, Flores M, Morse DC, Lodge TP. Apparent critical micelle concentrations in block copolymer/ionic liquid solutions: remarkably weak dependence on solvophobic block molecular weight. Macromolecules. 2012;45:4818–29.
45. Stoodley R, Wasan KM, Bizzotto D. Fluorescence of amphotericin B-deoxycholate (Fungizone) monomers and aggregates and the effect of heat-treatment. Langmuir. 2007;23:8718–25.
46. Barwicz J, Gruszecki WI, Gruda I. Spontaneous organization of amphotericin B in aqueous medium. J Colloid Interface Sci. 1993;158:71–6.
47. Jain JP, Kumar N. Development of amphotericin B loaded polymersomes based on (PEG)3-PLA co-polymers: factors affecting size and in vitro evaluation. Eur J Pharm Sci. 2010;40:456–65.
48. Ahmad Z, Shah A, Siddiq M, Kraatz H-B. Polymeric micelles as drug delivery vehicles. RSC Adv. 2014;4:17028–38.
49. Yu BG, Okano T, Kataoka K, Sardari S, Kwon GS. In vitro dissociation of antifungal efficacy and toxicity for amphotericin B-loaded poly(ethylene oxide)-block-poly(β-benzyl-L-aspartate) micelles. J Control Release. 1998;56:285–91.
50. Pujol I, Pastor FJ, dos Santos Lazéra M, Artigas JG. Evaluation of the Neo-Sensitabs® diffusion method for determining the antifungal susceptibilities of Cryptococcus gattii isolates, using three different agar media. Rev Iberoam Micol. 2008;25:215–20.
51. Ruiz HK, Serrano DR, Dea-Ayuela MA, Bilbao-Ramos PE, Bolás-Fernández F, Torrado JJ, et al. New amphotericin B-gamma cyclodextrin formulation for topical use with synergistic activity against diverse fungal species and Leishmania spp. Int J Pharm. 2014;473:148–57.